8. Hypogene Ore Characteristics

By Randolph A. Koski

8 of 21

Volcanogenic Massive Sulfide Occurrence Model

Scientific Investigations Report 2010–5070–C

U.S. Department of the Interior
U.S. Geological Survey

U.S. Department of the Interior
KEN SALAZAR, Secretary

U.S. Geological Survey
Marcia K. McNutt, Director

U.S. Geological Survey, Reston, Virginia: 2012

Suggested citation:
Koski, R.A., 2012, Hypogene ore characteristics in volcanogenic massive sulfide occurrence model: U.S. Geological Survey Scientific Investigations Report 2010–5070 –C, chap. 8, 10 p.

Contents

Figures

Tables

8. Hypogene Ore Characteristics

By Randolph A. Koski

Mineralogy

Although a detailed review of primary ore minerals in VMS deposits is beyond the scope of this report, a representative list of major, minor, and trace minerals culled from the literature is presented in table 8–1. The dominant ore mineralogy in most VMS deposits is relatively simple. In all deposit subtypes, the dominant sulfide mineral is pyrite or pyrrhotite. The next most abundant ore minerals, chalcopyrite and sphalerite, occur in variable amounts, and in a few deposits, one or the other or both occur in concentrations that exceed Fe sulfide content. The only other sulfide in the major mineral category is galena, which is concentrated in deposits associated with bimodal-felsic and siliciclastic-felsic rocks.

There are notable examples in which other ore minerals are abundant in VMS deposits. These include bornite at Kidd Creek (Hannington and others, 1999b) and Mount Lyell (Corbett, 2001); tetrahedrite, stibnite, and realgar in Au- and Ag-rich ores at Eskay Creek (Roth and others, 1999); arsenopyrite in Au-rich ore at Boliden (Weihed and others, 1996); and stannite and cassiterite in ore-grade tin mineralization at Neves Corvo and Kidd Creek (Hennigh and Hutchinson, 1999; Relvas and others, 2006). Table 8–1 includes a distinctive suite of Co- and Ni-bearing arsenides, sulfarsenides, and sulfides (for example, skutterudite, safflorite, cobaltite, löllingite, millerite, and pentlandite) that are rare in most VMS deposits, but relatively abundant in massive sulfide deposits associated with serpentinized ultramafic rocks in ophiolitic terranes of Quebec (Auclair and others, 1993), Morocco (Ahmed and others, 2009), and Cyprus (Thalhammer and others, 1986), as well as metaperidotites of the Outokumpu mining district in Finland (Peltonen and others, 2008). Potentially analogous VMS deposits associated with serpentinized ultramafic rocks on slow-spreading segments of the Mid-Atlantic Ridge (Rainbow, Logatchev) are also enriched in Co and Ni (Mozgova and others, 1999; Marques and others, 2006).

Although precious metals are an economically important commodity in many VMS deposits (Hannington and others, 1999c), they occur as volumetrically minor minerals. Visible gold is generally present as inclusions of native gold, electrum, or gold telluride minerals in major sulfide minerals, whereas silver occurs in Ag sulfides and sulfosalt minerals such as tetrahedrite and freibergite. In VMS-type mineralization on the modern seafloor, Au and Ag are most enriched in extensional arc and back-arc settings (Herzig and Hannington, 2000), although the mineralogy of gold is not yet well established. Occurrences of native gold as inclusions in sphalerite and chalcopyrite are reported in massive sulfide samples from Lau Basin and eastern Manus Basin (Herzig and others, 1993; Moss and Scott, 2001). Gold is also concentrated in massive sulfide deposits in Escanaba Trough, a slow-spreading segment of the Gorda Ridge. There, Törmänen and Koski (2005) have reported an association of native gold, electrum, and maldonite (Au_2Bi) with a suite of sulfarsenide and bismuth minerals.

Mineral Assemblages

The mineral assemblages (and bulk chemical characteristics) of VMS deposits are directly related to the chemistry of ore-forming hydrothermal fluids that, in turn, reflect exchange reactions with wall rocks during fluid circulation. Thus, massive sulfide deposits formed in predominantly mafic rock environments are likely to have discrete mineralogical differences from deposits associated with sequences of predominantly felsic rocks. Furthermore, mineral assemblages are also influenced by fluids whose compositions are altered during passage through substantial thicknesses of arc- or continent-derived sediment. Whatever the source rocks, variations in mineralogy are often most obvious in the minor and trace mineral assemblages. A few examples are cited to illustrate variations in VMS mineral assemblages that correspond to a range of host-rock compositions.

Volcanogenic massive sulfide deposits occurring in mafic volcanic rocks are characterized by a major-mineral assemblage dominated by pyrite (much less frequently pyrrhotite or marcasite) along with variable but subordinate amounts of chalcopyrite and sphalerite (Galley and Koski, 1999). Other sulfide minerals are present in trace amounts, and more significantly, galena and base-metal sulfosalts are rare in all parts of these deposits. Deposits in siliciclastic-mafic environments have similar lead-poor mineral assemblages; however, pyrrhotite is more abundant relative to pyrite in some deposits (Slack, 1993; Peter and Scott, 1999). At the other end of the lithologic spectrum in which rhyolites and dacites are predominant, VMS deposits (such as Kuroko deposits) contain abundant and variable amounts of pyrite, chalcopyrite, and sphalerite, along with significant galena and tetrahedrite (Eldridge

Table 8–1. Hypogene ore mineralogy of volcanogenic massive sulfide deposits.

[Sources: Franklin and others, 1981; Large, 1992; Slack, 1993; Hannington and others, 1999a, e; Peter and Scott, 1999; Slack and others, 2003; Herrington and others, 2005; Koski and others, 2008; Peltonen and others, 2008; Ahmed and others, 2009]

Major minerals	
pyrite	FeS_2
pyrrhotite	$Fe_{1-X}S$
chalcopyrite	$CuFeS_2$
sphalerite	(Zn, Fe)S
galena	ZnS
Minor minerals	
marcasite	FeS_2
magnetite	Fe_3O_4
cobaltite	(Co, Fe)AsS
arsenopyrite	FeAsS
tennantite	$Cu_{12}As_4S_{13}$
tetrahedrite	$Cu_{12}Sb_4S_{13}$
Trace minerals	
acanthite	Ag_2S
argentite	Ag_2S
bismuth	Bi
bismuthinite	Bi_2S_3
bismuth tellurides	Bi_2Te_3
bornite	Cu_5FeS_4
cubanite	$CuFe_2S_3$
boulangerite	$Pb_5Sb_4S_{11}$
bournonite	$PbCuSbS_3$
brannerite	UTi_2O_6
bravoite	$(Fe, Ni, Co)S_2$
carrolite	$CuCo_2S_4$
cassiterite	SnO_2
cinnabar	HgS
electrum	(Au, Ag)
digenite	Cu_9S_5
enargite	Cu_3AsS_4

Trace minerals (cont.)	
freibergite	$(Ag, Cu)_{12}(Sb, As)_4S_{13}$
germanite	$Cu_3(Ge, Fe)(S, As)_4$
gersdorffite	NiAsS
glaucodot	(Co,Fe)AsS
gold	Au
gold tellurides	
idaite	Cu_5FeS_6
hedleyite	Bi_7Te_3
hessite	Ag_2Te
löllingite	$FeAs_2$
mackinawite	Fe_1+XS
millerite	NiS
mawsonite	$Cu_6Fe_2SnS_8$
molybdenite	MoS_2
nickeline	NiAs
pentlandite	$(Fe, Ni)_9S_8$
pyrargyrite	Ag_3SbS_3
realgar	AsS
rammelsbergite	$NiAs_2$
roquesite	$CuInS_2$
rutile	TiO_2
safflorite	$CoAs_2$
silver	Ag
skutterudite	$CoAs_{2-3}$
stannite	Cu2FeSnS4
stibnite	Sb_2S_3
stromeyerite	AgCuS
tetradymite	Bi_2Te_2S
valleriite	$(Fe, Cu)S_2 \bullet (Mg, Al)(OH)_2$
wurtzite	ZnS

and others, 1983). Deposits having this lithologic association often contain zones of ore with sulfide assemblages dominated by sphalerite and galena (for example, Rosebery; Smith and Huston, 1992), and in rare instances, ore mineral assemblages dominated by galena, tetrahedrite, realgar, and stibnite (Eskay Creek; Roth and others, 1999). Massive sulfide deposits in bimodal volcanic sequences can be expected to have sulfide mineral assemblages somewhat intermediate between mafic- and felsic-rock endmembers. Thus, the major mineral suite of pyrite, pyrrhotite, sphalerite, and chalcopyrite at Bald Mountain contains minor but significant galena and arsenopyrite mineralization within the orebody (Slack and others, 2003).

Paragenesis

Paragenesis, the sequence of mineral deposition, is complicated by replacement of early-formed minerals by new minerals as temperature conditions wax and wane during ongoing hydrothermal activity. Studies of contemporary "black smoker" massive sulfide chimneys and mounds on ocean ridges provide the best record of temporal mineralogical changes during formation of VMS deposits. Although mineral paragenesis will vary somewhat from deposit to deposit and within a given deposit, a generalized depositional sequence for major sulfide, sulfate, and silica minerals within a hypothetical sulfide chimney is shown in figure 8–1*A* (Hannington and others, 1995). At temperatures up to about 250 °C, barite, anhydrite, silica, sphalerite, and marcasite are precipitated. When temperature increases to about 350 °C, these minerals are replaced by pyrite, wurtzite, chalcopyrite, pyrrhotite, and isocubanite. An important aspect of this sequence is the replacement of original sulfides by Cu-Fe sulfides and pyrrhotite at high temperature. Sulfate and silicate mineral phases along with sphalerite and marcasite/pyrite are also deposited in late stages of mineralization as fluid temperatures decrease.

Mineral paragenesis for ancient VMS deposits can be much more complicated than that for the seafloor chimney cited above. A paragenetic diagram for the principal hypogene sulfide minerals (plus quartz) in the massive sulfide deposit at Bald Mountain is presented in figure 8–1*B* (Slack and others, 2003). The diagram for Bald Mountain illustrates a complex and repetitive pattern of sulfide mineral deposition during multiple stages of deposit formation. A noteworthy similarity between the Bald Mountain and seafloor chimney paragenesis, however, is the early Stage 1 deposition of pyrite, marcasite, sphalerite, and quartz followed by pyrrhotite and chalcopyrite replacement at higher temperatures in Stage 2. Numerous additional stages of mineral precipitation, mostly in the form of crosscutting veins, are superimposed on the massive pyrrhotite-chalcopyrite mineralization at Bald Mountain (Slack and others, 2003). The paragenesis of hypogene ore minerals in many ancient VMS deposits is further complicated by recrystallization and replacement during posthydrothermal metamorphism (for example, bornite ores at Kidd Creek; Hannington and others, 1999b).

Zoning Patterns

A deposit-scale zonation pattern in which the upper stockwork is dominated by chalcopyrite + pyrite ± magnetite, the basal part of the massive sulfide body is dominated by pyrite + chalcopyrite, and the upper and outer margins of the massive sulfide are dominated by sphalerite ± galena (± barite) has long been recognized in VMS systems (Lambert and Sato, 1974; Large, 1977; Eldridge and others, 1983). A highly idealized version of this zonation pattern (modified from Lydon, 1984)—including hypogene ore minerals in the massive sulfide lens and stockwork along with related stockwork alteration and peripheral sedimentary deposits—is illustrated in figure 8–2. This basic pattern of vertical zoning is best exhibited in well preserved deposits having bimodal-felsic or bimodal-mafic affinities (table 8–2) and has been attributed to sequential episodes of sulfide deposition and replacement within an intensifying geothermal system by Eldridge and others (1983) and Pisutha-Arnond and Ohmoto (1983). In their models, increasing fluid temperatures at the base of the growing ore lens result in chalcopyrite replacement of an earlier sulfide facies dominated by sphalerite, tetrahedrite, galena, and pyrite. The mobilized Zn and Pb migrate upward and reprecipitate as sphalerite and galena in cooler parts of the lens, resulting in the zonation of chalcopyrite and sphalerite (±galena) and Cu and Zn (±Pb) in many VMS deposits. The outward movement or "zone refining" of metals may also produce Au enrichment in sphalerite-rich zones of VMS deposits (Hannington and others, 1986; Large and others, 1989). Conversely, the very low base- and precious-metal concentrations in pyritic, ophiolite-hosted VMS deposits located in Cyprus and Oman may reflect the complete stripping or "over refining" of metals during sustained hydrothermal activity on the paleoseafloor (Hannington and others, 1998).

Deposit-scale zonation of Cu and Zn sulfides has also been described in massive sulfide mounds constructed on mid-ocean ridges (Embley and others, 1988; Fouquet and others, 1993). Perhaps the most distinctive example of Cu-Zn zoning is observed in individual high-temperature (>300 °C) black smoker chimneys (fig. 8–3) forming in contemporary ridge settings (Haymon, 1983; Goldfarb and others, 1983; Koski and others, 1994). In these examples, the precipitation of chalcopyrite and sphalerite is controlled by extreme temperature and chemical gradients operating at the centimeter scale.

Textures and Structures

Volcanogenic massive sulfide deposits span a continuum of physical attributes from massive ores composed of 100 percent sulfide minerals through semimassive ores that are mixtures of sulfides, gangue minerals, and host rock (volcanic or sedimentary) to increasingly sparse sulfide disseminated in wall rocks. This gradation may represent a vertical transition from seafloor (or near seafloor) mineralization to mineralization at depth within the feeder zone of the hydrothermal

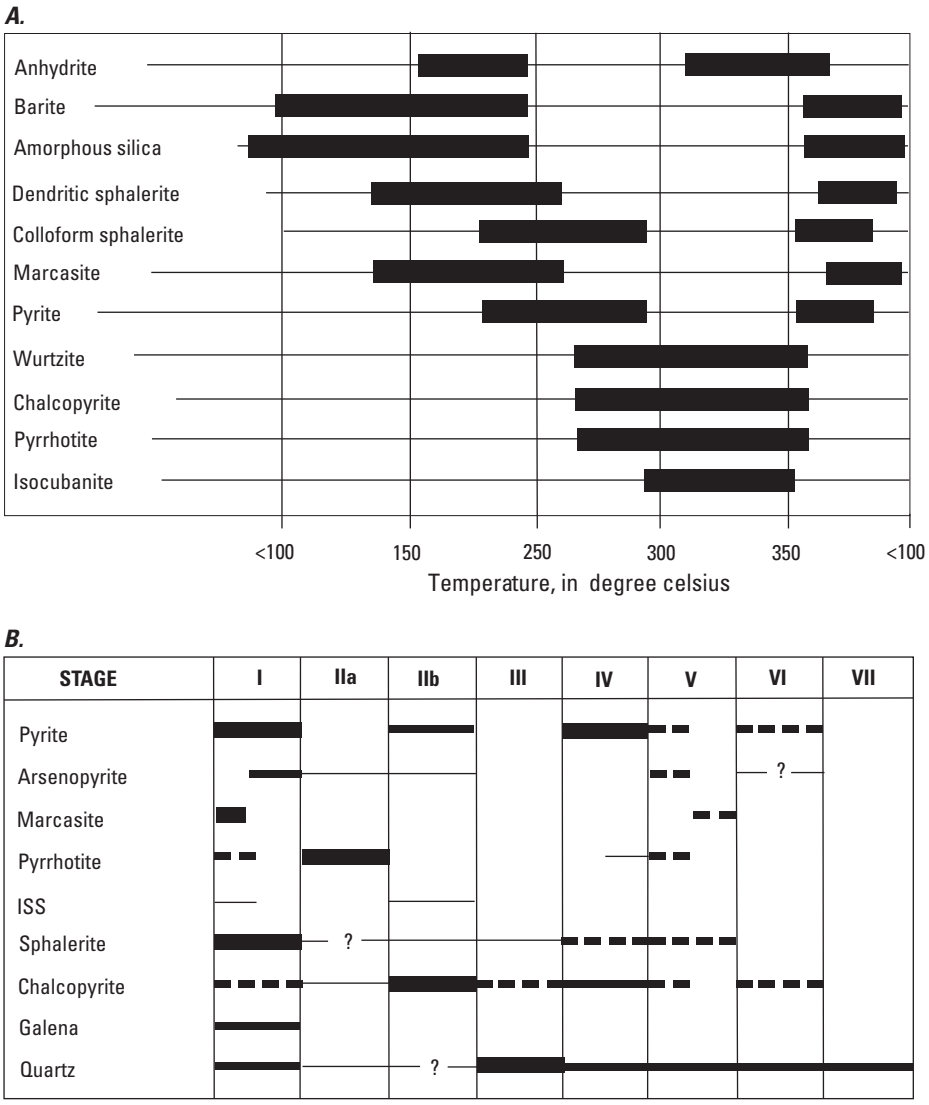

Figure 8–1. Examples of paragenetic sequences in volcanogenic massive sulfide deposits. *A*, Mineral paragenesis in hypothetical sulfide-sulfate-silica chimney. From Hannington and others (1995). During chimney growth, fluid temperatures increase to approximately 350 °C and then decrease as hydrothermal fluids mix with seawater. *B*, Paragenesis of hypogene sulfide minerals and quartz at Bald Mountain (Maine) massive sulfide deposit. After Slack and others (2003). Thickness of black bars represents relative proportions of minerals. [ISS, intermediate solid solution in the copper-iron-sulfur system]

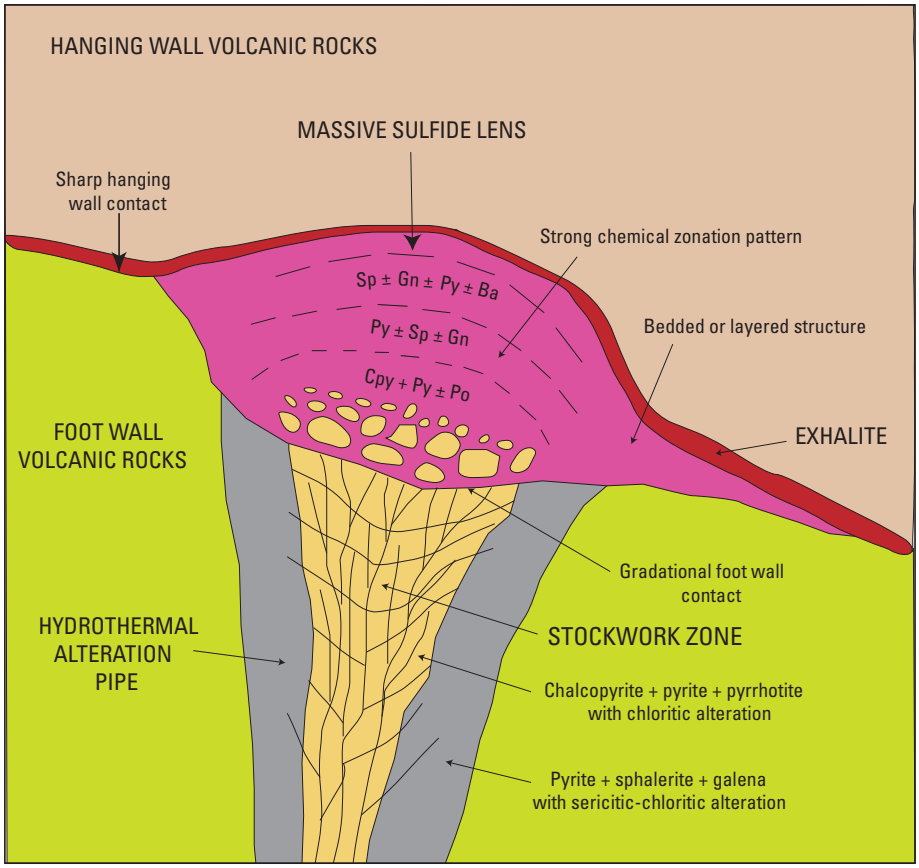

Figure 8–2. Idealized massive sulfide lens illustrating zonation features for hypogene ore minerals. Modified from Lydon (1984). [ba, barite; cpy, chalcopyrite; gn, galena; po, pyrrhotite; py, pyrite; sp, sphalerite]

Table 8–2. Examples of hypogene mineral zonation patterns in selected volcanogenic massive sulfide deposits.

[Cu, copper; Zn, zinc; ba, barite; bn, bornite; ch, chlorite; cp, chalcopyrite; gl, galena; mt, magnetite; po, pyrrhotite; py, pyrite; sp, sphalerite; ten, tennantite]

Deposit or district	Mineral zonation	Reference
Hokuroku district (composite)	Top to bottom: Barite ore: ba > sulfides Massive black ore: sp + ba> py + gl Semiblack ore: sp + ba > py > cp Massive yellow ore: ch + py Powdery yellow ore: py > cp Massive pyrite ore: py >> cp >> sp	Eldridge and others (1983)
Silver Peak (Oregon, USA)	Top to bottom: Barite ore: ba Black ore: py + bn + ten + sp + ba ± cp Yellow ore: py + cp + bn Friable yellow ore: py	Derkey and Matsueda (1989)
Urals Cu-Zn deposit (composite)	Top to bottom: Outer/upper massive sulfide: sp + py ± cp ± ba ± gl Middle massive sulfide: cp + py Stockwork and basal massive sulfide: cp + py ± po ± mt	Herrington and others (2005)
Bathurst camp (composite)	Distal to proximal: Bedded pyrite: py ± sp ± gl Bedded ores: py + sp + gl ± cp Ore-vent complex: po + mt + py + cp ± sp ± gl	Goodfellow and McCutcheon (2003)

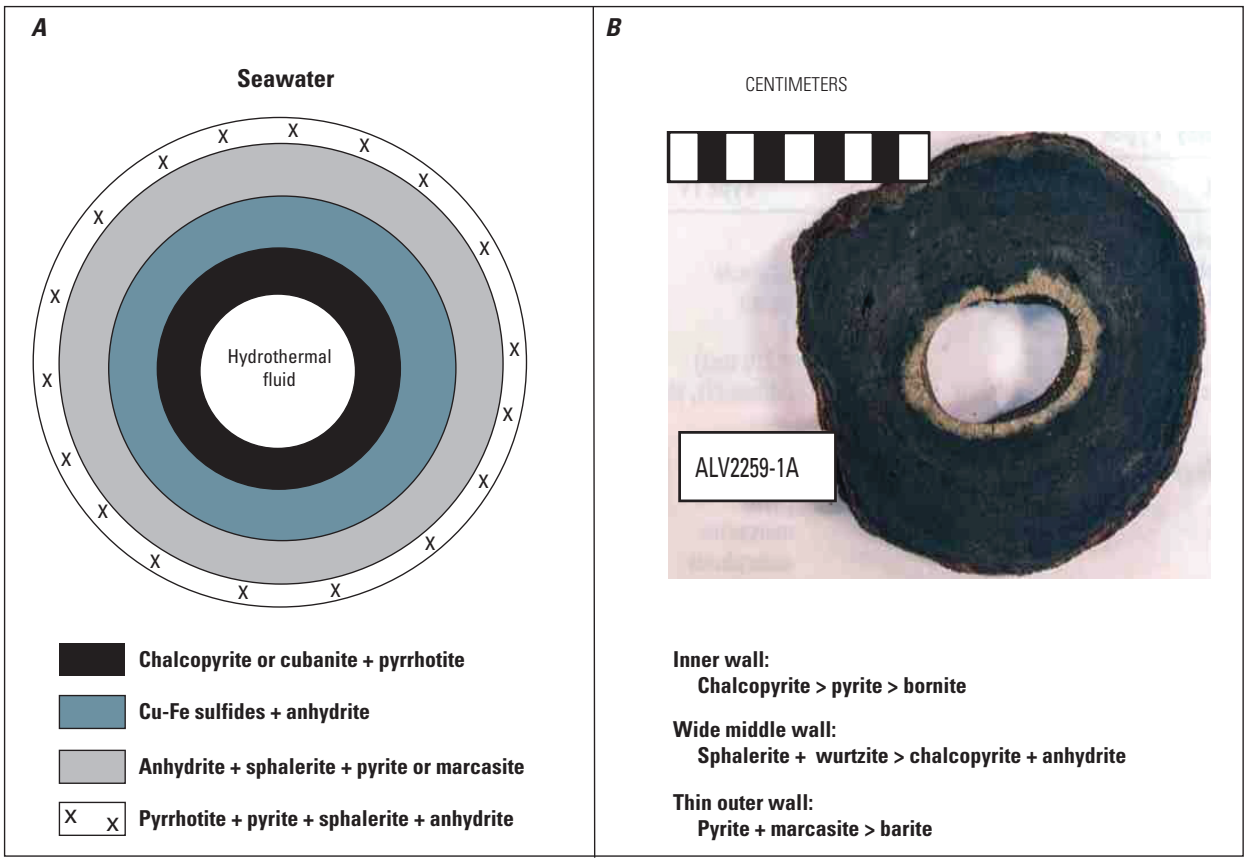

Figure 8–3. Comparative hypogene mineral zonation in (*A*) model of a 350°C "black smoker" chimney from the East Pacific Rise, 21°N (after Haymon, 1983), and (*B*) cross section of high temperature (approx. 310°C) chimney from Monolith Vent, southern Juan de Fuca Ridge (from Koski and others, 1994). Each chimney has an inner wall dominated by copper-iron sulfides, a middle wall containing abundant zinc sulfides, and an outer rind dominated by iron sulfides. [Cu, copper; Fe, iron]

system (for example, Turner-Albright; Zierenberg and others, 1988). Sulfide minerals also form veins (usually with quartz and other gangue minerals) cutting wall rock and earlier-formed massive sulfides, and many massive sulfide bodies are underlain by discordant vein networks (stockwork zones). Massive sulfides in many deposits are laterally gradational to bedded or layered sulfide deposits formed by mass wasting of the elevated mounds on the seafloor.

At the hand-specimen and thin section scale, massive sulfides are typically compact, fine-grained aggregates of intergrown sulfide minerals with irregular grain boundaries. More diagnostic primary textures in massive ores include idiomorphic crystals (for example, pyrite, pyrrhotite) projecting into cavities, colloform overgrowths (especially sphalerite, pyrite, and marcasite), framboidal and botryoidal pyrite, pseudomorphic replacement (for example, sulfate by pyrrhotite), fine-scale replacement relationships (for example, chalcopyrite disease in sphalerite; Barton and Bethke, 1987), boxwork intergrowths, and internal mineral growth zoning (especially in Zn sulfides). Other common attributes of unmetamorphosed ores are high porosity and textural heterogeneity on the thin section scale. These types of primary textural features are especially well preserved in modern seafloor deposits (see Koski and others, 1984; Paradis and others, 1988; Hannington and others, 1995).

Textures and structures in ancient VMS deposits typically bear some overprint of postdepositional diagenesis and metamorphism. Metamorphism causes numerous textural changes including (1) recrystallization and increase in grain size, (2) development of porphyroblasts, (3) foliation and alignment of sulfide and gangue crystals, (4) 120° triple junction grain boundaries (annealing textures), (5) remobilization

of chalcopyrite, and (6) penetrative deformation ("durchbewegung" texture) of pyrrhotite and wall rock (Vokes, 1969; Franklin and others, 1981).

Most VMS deposits exhibit some form of primary structure. Fragmental and layered ores are prevalent structural characteristics at the deposit scale (see Spense, 1975; Slack and others, 2003; Tornos, 2006). In many cases, these features appear to result from mass wasting and flow from the steep flanks of sulfide mounds. Mass wasting and proximal sedimentation of hydrothermal debris from the TAG sulfide mound on the Mid-Atlantic Ridge represent a useful modern analog (Mills and Elderfield, 1995). Blocky, fragmental, and sandy zones also form distinctive internal structural features of well preserved massive sulfides (Constantinou, 1976; Eldridge and others, 1983; Lydon and Galley, 1986). Studies of contemporary seafloor sulfide mounds, especially the TAG site, indicate that these breccias formed by collapse of unstable sulfide chimneys on the mound surface as well as collapse following anhydrite dissolution in the core of the mound structure (Humphris and others, 1995; Petersen and others, 2000). Less common primary structures preserved in some VMS deposits include chimney fragments with fluid channelways (Oudin and Constantinou, 1984; Slack and others, 2003), fossils of hydrothermal vent fauna (Haymon and others, 1984; Little and others, 1999), and traces of microbial life forms (Juniper and Fouquet, 1988).

Grain Size

Volcanogenic massive sulfide deposits are typically fine grained. The range in grain sizes for the major hypogene sulfide minerals in unmetamorphosed massive sulfide deposits is approximately 0.1–1 millimeter (mm); accessory sulfides are considerably smaller in size. The grain size of gold minerals is smaller than that of major sulfides by more than one order of magnitude. In one example, the median size values for discrete gold grains (electrum) in eleven eastern Australian VMS deposits lie between 2.5 and 25 micrometers (mm) (Huston and others, 1992). In contrast, metamorphosed massive sulfides are coarser grained; sulfide grains in metamorphosed deposits commonly exceed 1 mm in diameter, and pyrite porphyroblasts up to 300 mm across occur in pyrrhotite-rich ores of the Ducktown mining district, Tennessee (Brooker and others, 1987).

References Cited

Ahmed, A.H., Arai, S., and Ikenne, M., 2009, Mineralogy and paragenesis of the Co-Ni arsenide ores of Bou Azzer, Anti-Atlas, Morocco: Economic Geology, v. 104, p. 249–266.

Auclair, M., Gauthier, M., Trottier, J., Jébrak, M., and Chartrand, F., 1993, Mineralogy, geochemistry, and paragenesis of the Eastern Metals serpentinite-associated Ni-Cu-Zn deposit, Quebec Appalachians: Economic Geology, v. 88, p. 123–138.

Barton, P.B., Jr., and Bethke, P.M., 1987, Chalcopyrite disease in sphalerite—Pathology and epidemiology: American Mineralogist, v. 72, p. 451–467.

Brooker, D.D., Craig, J.R., and Rimstidt, J.D., 1987, Ore metamorphism and pyrite porphyroblast development at the Cherokee mine, Ducktown, Tennessee: Economic Geology, v. 82, p. 72–86.

Constantinou, G., 1976, Genesis of conglomerate structure, porosity and collomorphic textures of the massive sulphide ores of Cyprus, in Strong, D.F., ed., Metallogeny and plate tectonics: Geological Association of Canada Special Paper 14, p. 187–210.

Corbett, K.D., 2001, New mapping and interpretations of the Mount Lyell mining district, Tasmania—A large hybrid Cu-Au system with an exhalative Pb-Zn top: Economic Geology, v. 96, p. 1089–1122.

Derkey, R.E., and Matsueda, H., 1989, Geology of the Silver Peak mine, a Kuroko-type deposit in Jurassic volcanic rocks, Oregon, U.S.A.: Journal of the Mining College of Akita University, ser. A, v. VII, no. 2, p. 99–123.

Eldridge, C.S., Barton, P.B., Jr., and Ohmoto, H., 1983, Mineral textures and their bearing on formation of the Kuroko orebodies, in Ohmoto, H., and Skinner, B.J., eds., The Kuroko and related volcanogenic massive sulfide deposits: Economic Geology Monograph 5, p. 241–281.

Embley, R.W., Jonasson, I.R., Perfit, M.R., Franklin, J.M., Tivey, M.A., Malahoff, A., Smith, M.F., and Francis, T.J.G, 1988, Submersible investigation of an extinct hydrothermal system on the Galapagos Ridge—Sulfide mounds, stockwork zone, and differentiated lavas: Canadian Mineralogist, v. 26, p. 517–539.

Fouquet, Y., Wafic, A., Cambon, P., Mevel, C., Meyer, G., and Gente, P., 1993, Tectonic setting and mineralogical and geochemical zonation in the Snake Pit sulfide deposit (Mid-Atlantic Ridge at 23°N): Economic Geology, v. 88, p. 2018–2036.

Franklin, J.M., Lydon, J.M., and Sangster, D.F., 1981, Volcanic-associated massive sulfide deposits, in Skinner, B.J., ed., Economic Geology 75th anniversary volume, 1905–1980: Littleton, Colo., Economic Geology Publishing Company, p. 485–627.

Galley, A.G., and Koski, R.A., 1999, Setting and characteristics of ophiolite-hosted volcanogenic massive sulfide deposits, in Barrie, C.T., and Hannington, M.D., Volcanic-associated massive sulfide deposits—Processes and examples in modern and ancient settings: Reviews in Economic Geology, v. 8, p. 221–246.

Goldfarb, M.S., Converse, D.R., Holland, H.D., and Edmond, J.M., 1983, The genesis of hot spring deposits on the East Pacific Rise, 21°N, in Ohmoto, H., and Skinner, B.J., eds., The Kuroko and related volcanogenic massive sulfide deposits: Economic Geology Monograph 5, p.184–197.

Goodfellow, W.D., and McCutcheon, S.R., 2003, Geologic and genetic attributes of volcanic sediment-hosted massive sulfide deposits of the Bathurst mining camp, New Brunswick—A synthesis, in Goodfellow, W.D., McCutcheon, S.R., and Peter, J.M., eds., Massive sulfide deposits of the Bathurst mining camp, New Brunswick, and northern Maine: Economic Geology Monograph 11, p. 245–301.

Hannington, M.D., Bleeker, W., and Kjarsgaard, I., 1999a, Sulfide mineralogy, geochemistry, and ore genesis of the Kidd Creek deposit—Part I. North, central, and south orebodies, in Hannington, M.D., and Barrie, C.T., eds., The giant Kidd Creek volcanogenic massive sulfide deposit, western Abitibi subprovince, Canada: Economic Geology Monograph 10, p. 163–224.

Hannington, M.D., Bleeker, W., and Kjarsgaard, I., 1999b, Sulfide mineralogy, geochemistry, and ore genesis of the Kidd Creek deposit—Part II. The bornite zone, in Hannington, M.D., and Barrie, C.T., eds., The giant Kidd Creek volcanogenic massive sulfide deposit, western Abitibi subprovince, Canada: Economic Geology Monograph 10, p. 225–266.

Hannington, M.D., Galley, A.G., Herzig, P.M., and Petersen, S., 1998, Comparison of the TAG mound and stockwork complex with Cyprus-type massive sulfide deposits, in Herzig, P.M., Humphris, S.E., Miller, D.J., and Zierenberg, R.A., eds., TAG—Drilling an active hydrothermal system on a sediment-free slow-spreading ridge, site 957: Proceedings of the Ocean Drilling Program, Scientific Results, v. 158, p. 389–415.

Hannington, M.D., Jonasson, I.R., Herzig, P.M., and Petersen, S., 1995, Physical and chemical processes of seafloor mineralization, in Humphris, S.E., Zierenberg, R.A., Mullineaux, L.S., and Thomson, R.E., eds., Seafloor hydrothermal systems—Physical, chemical, biological, and geological interactions: American Geophysical Union Geophysical Monograph 91, p. 115–157.

Hannington, M.D., Peter, J.M., and Scott, S.D., 1986, Gold in sea-floor polymetallic sulfide deposits: Economic Geology, v. 81, p. 1867–1883.

Hannington, M.D., Poulsen, K.H., Thompson, J.F.H., and Sillitoe, R.H., 1999c, Volcanogenic gold in the massive sulfide environment, in Barrie, C.T., and Hannington, M.D., eds., Volcanic-associated massive sulfide deposits—Processes and examples in modern and ancient settings: Reviews in Economic Geology, v. 8, p. 325–356.

Haymon, R.M., 1983, Growth history of hydrothermal black smoker chimneys: Nature, 301, p. 695–698.

Haymon, R.M., Koski, R.A., and Sinclair, C., 1984, Fossils of hydrothermal vent worms discovered in Cretaceous sulfide ores of the Samail ophiolite, Oman: Science, v. 223, p. 1407–1409.

Hennigh, Q., and Hutchinson, R.W., 1999, Cassiterite at Kidd Creek—An example of volcanogenic massive sulfide-hosted tin mineralization, in Hannington, M.D., and Barrie, C.T., eds., The giant Kidd Creek volcanogenic massive sulfide deposit, western Abitibi subprovince, Canada: Economic Geology Monograph 10, p. 431–440.

Herrington, R.J., Maslennikov, V., Zaykov, V., Seravkin, I., Kosarev, A., Buschmann, B., Orgeval, J.-J., Holland, N., Tesalina, S., Nimis, P., and Armstrong, R., 2005, Classification of VMS deposits—Lessons from the South Uralides: Ore Geology Reviews, v. 27, p. 203–237.

Herzig, P.M., and Hannington, M.D., 2000, Polymetallic massive sulfides and gold mineralization at mid-ocean ridges and in subduction-related environments, in Cronan, D.S., ed., Handbook of marine mineral deposits: Boca Raton, Fla., CRC Press Marine Science Series, p. 347–368.

Herzig, P.M., Hannington, M.D., Fouquet, Y., von Stackelberg, U., and Petersen, S., 1993, Gold-rich polymetallic sulfides from the Lau back arc and implications for the geochemistry of gold in sea-floor hydrothermal systems of the southwest Pacific: Economic Geology, v. 88, p. 2182–2209.

Humphris, S.E., Herzig, P.M., Miller, D.J., Alt, J.C., Becker, K., Brown, D., Brugmann, G., Chiba, H., Fouquet, Y., Gemmell, J.B., Guerin, G., Hannington, M.D., Holm, N.G., Honnorez, J.J., Iturrino, G.J., Knott, R., Ludwig, R., Nakamura, K., Petersen, S., Reysenbach, A.L., Rona, P.A., Smith, S., Sturz, A.A., Tivey, M.K., and Zhao, X., 1995, The internal structure of an active sea-floor massive sulphide deposit: Nature, v. 377, no. 6551, p. 713–716.

Huston, D.L., Bottrill, R.S., Creelman, R.A., Zaw, K., Ramsden, T.R., Rand, S.W., Gemmell, J.B., Jablonski, W., Sie, S.H., and Large, R.R., 1992, Geologic and geochemical controls on the mineralogy and grain size of gold-bearing phases, eastern Australian volcanic-hosted massive sulfide deposits: Economic Geology, v. 87, p. 542–563.

Juniper, S.K., and Fouquet, Y., 1988, Filamentous iron-silica deposits from modern and ancient hydrothermal sites: The Canadian Mineralogist, v. 26, p. 859–869.

Koski, R.A., Clague, D.A., and Oudin, E., 1984, Mineralogy and chemistry of massive sulfide deposits from the Juan de Fuca Ridge: Geological Society of America Bulletin, v. 95, p. 930–945.

Koski, R.A., Jonasson, I.R., Kadko, D.C., Smith, V.K., and Wong, F.L., 1994, Compositions, growth mechanisms, and temporal relations of hydrothermal sulfide-sulfate-silica chimneys at the northern Cleft segment, Juan de Fuca Ridge: Journal of Geophysical Research, v. 99, p. 4813–4832.

Koski, R.A., Munk, L., Foster, A.L., Shanks, W.C., III, and Stillings, L.L., 2008, Sulfide oxidation and distribution of metals near abandoned copper mines in coastal environments, Prince William Sound, Alaska, USA: Applied Geochemistry, v. 23, p. 227–254.

Lambert, I.B., and Sato, T., 1974, The Kuroko and associated ore deposits of Japan—A review of their features and metallogenesis: Economic Geology, v. 69, p. 1215–1236.

Large, R.R., 1977, Chemical evolution and zonation of massive sulfide deposits in volcanic terrains: Economic Geology, v. 72, p. 549–572.

Large, R.R., 1992, Australian volcanic-hosted massive sulfide deposits—Features, styles, and genetic models: Economic Geology, v. 87, p. 471–510.

Large, R.R., Huston, D.L., McGoldrick, P.J., Ruxton, P.A., and McArthur, G., 1989, Gold distribution and genesis in Australian volcanogenic massive sulfide deposits and their significance for gold transport models, in Keays, R.R., Ramsay, W.R.H., and Groves, D.I., eds., The geology of gold deposits—The perspective in 1988: Economic Geology Monograph 6, p. 520–535.

Little, C.T.S., Cann, J.R., Herrington, R.J., and Morisseau, M., 1999, Late Cretaceous hydrothermal vent communities from the Troodos ophiolite, Cyprus: Geology, v. 27, p. 1027–1030.

Lydon, J.W., 1984, Volcanogenic massive sulphide deposits—Part 1. A descriptive model: Geoscience Canada, v. 11, p. 195–202.

Lydon, J.W., and Galley, A.G., 1986, Chemical and mineralogical zonation of the Mathiati alteration pipe, Cyprus, and its genetic significance, in Gallagher, M.J., Ixer, R.A., Neary, C.R., and Prichard, H.M., eds., Metallogeny of basic and ultrabasic rocks: London Institute of Mining and Metallurgy, p. 46–68.

Marques, A.F.A., Barriga, F., Chavagnac, V., and Fouquet, Y., 2006, Mineralogy, geochemistry, and Nd isotope composition of the Rainbow hydrothermal field, Mid-Atlantic Ridge: Mineralium Deposita, v. 41, p. 52–67.

Mills, R.A., and Elderfield, H., 1995, Hydrothermal activity and the geochemistry of metalliferous sediment, in Humphris, S.E., Zierenberg, R.A., Mullineaux, L.S., and Thomson, R.E., eds., Seafloor hydrothermal systems—Physical, chemical, biological, and geological interactions: American Geophysical Union, Geophysical Monograph 91, p. 392–407.

Moss, R., and Scott, S.D., 2001, Geochemistry and mineralogy of gold-rich hydrothermal precipitates from the eastern Manus Basin, Papua New Guinea: Canadian Mineralogist, v. 39, p. 957–978.

Mozgova, N.N., Efimov, A., Borodaev, Y.S., Krasnov, S.G., Cherkashov, G.A., Stepanova, T.V., and Ashadze, A.M., 1999, Mineralogy and chemistry of massive sulfides from the Logatchev hydrothermal field (14 degrees 45'N Mid-Atlantic Ridge): Exploration and Mining Geology, v. 8, p. 379–395.

Oudin, E., and Constantinou, G., 1984, Black smoker chimney fragments in Cyprus sulphide deposits: Nature, v. 308, p. 349–353.

Paradis, S., Jonasson, I.R., Le Cheminant, G.M., and Watkinson, D.H., 1988, Two zinc-rich chimneys from the Plume Site, southern Juan de Fuca Ridge: Canadian Mineralogist, v. 26, p. 637–654.

Peltonen, P., Kontinen, A., Huhma, H., and Kuronen, U., 2008, Outokumpu revisited—New mineral deposit model for the mantle peridotite-associated Cu-Co-Zn-Ni-Ag-Au sulphide deposits: Ore Geology Reviews, v. 33, p. 559–617.

Peter, J.M., and Scott, S.D., 1999, Windy Craggy, northwestern British Columbia—The world's largest Besshi-type deposit, in Barrie, C.T., and Hannington, M.D., eds., Volcanic-associated massive sulfide deposits—Processes and examples in modern and ancient settings: Reviews in Economic Geology, v. 8, p. 261–295.

Petersen, S., Herzig, P.M., and Hannnington, M.D., 2000, Third dimension of a presently forming VMS deposit—TAG hydrothermal mound, Mid-Atlantic Ridge, 26°N: Mineralium Deposita, v. 35, p. 233–259.

Pisutha-Arnond, V., and Ohmoto, H., 1983, Thermal history and chemical and isotopic compositions of the ore-forming fluids responsible for the Kuroko massive sulfide deposits in the Hokuroku District of Japan, in Ohmoto, H., and Skinner, B.J., eds., The Kuroko and related volcanogenic massive sulfide deposits: Economic Geology Monograph 5, p. 523–558.

Relvas, J.M.R.S., Barriga, J.A.S., Ferreira, A., Noiva, P.C., Pacheco, N., and Barriga, G., 2006, Hydrothermal alteration and mineralization in the Neves-Corvo volcanic-hosted massive sulfide deposit, Portugal—Part I. Geology, mineralogy, and geochemistry: Economic Geology, v. 101, p. 753–790.

Roth, T., Thompson, J.F.H., and Barrett, T.J., 1999, The precious metal-rich Eskay Creek deposit, northwestern British Columbia, in Barrie, C.T., and Hannington, M.D., eds., Volcanic-associated massive sulfide deposits—Processes and examples in modern and ancient settings: Reviews in Economic Geology, v. 8, p. 357–373.

Slack, J.F., 1993, Descriptive and grade-tonnage models for Besshi-type massive sulphide deposits, in Kirkham, R.V., Sinclair, W.D., Thorpe, R.I., and Duke, J.M., eds., Mineral deposit modeling: Geological Association of Canada Special Paper 40, p. 343–371.

Slack, J.F., Foose, M.P., Flohr, M.J.K., Scully, M.V., and Belkin, H.E., 2003, Exhalative and subseafloor replacement processes in the formation of the Bald Mountain massive sulfide deposit, northern Maine, in Goodfellow, W.D., McCutcheon, S.R., and Peter, J.M., eds., Volcanogenic massive sulfide deposits of the Bathurst district, New Brunswick, and northern Maine: Economic Geology Monograph 11, p. 513–548.

Smith, R.N., and Huston, D.L., 1992, Distribution and association of selected trace elements at the Rosebery deposit, Tasmania: Economic Geology, v. 87, p. 706–719.

Spence, C.D., 1975, Volcanogenic features of the Vauze sulfide deposit, Noranda, Quebec: Economic Geology v. 70, p. 102–114.

Thalhammer, O., Stumpfl, E.F., and Panayiotou, A., 1986, Postmagmatic, hydrothermal origin of sulfide and arsenide mineralizations at Limassol Forest, Cyprus: Mineralium Deposita, v. 21, p. 95–105.

Törmänen, T.O., and Koski, R.A., 2005, Gold enrichment and the Bi-Au association in pyrrhotite-rich massive sulfide deposits, Escanaba Trough, southern Gorda Ridge: Economic Geology, v. 100, p. 1135–1150.

Tornos, F., 2006, Environment of formation and styles of volcanogenic massive sulfides—The Iberian Pyrite Belt: Ore Geology Reviews, v. 28, p. 259–307.

Vokes, F.M., 1969, A review of the metamorphism of sulfide deposits: Earth Science Reviews, v. 5, p. 99–143.

Weihed, J.B., Bergström, U., Billström, K., and Weihed, P., 1996, Geology, tectonic setting and origin of the PaleoProterozoic Boliden Au-Cu-As deposit, Skellefte District, northern Sweden: Economic Geology, v. 91, p. 1073–1097.

Zierenberg, R.A., Shanks, W.C., III, Seyfried, W.E., Jr., Koski, R.A., and Strickler, M.D., 1988, Mineralization, alteration, and hydrothermal metamorphism of the ophiolite-hosted Turner-Albright sulfide deposit, southwestern Oregon: Journal of Geophysical Research, v. 93, p. 4657–4674.